

# Reducing Boolean Networks with Backward Boolean Equivalence - extended version<sup>\*</sup>

Georgios Argyris<sup>1</sup>[0000-0002-3203-0410], Alberto Lluch  
Lafuente<sup>1</sup>[0000-0001-7405-0818], Mirco Tribastone<sup>2</sup>[0000-0002-6018-5989], Max  
Tschaikowski<sup>3</sup>[0000-0002-6186-8669], and Andrea Vandin<sup>4,1</sup>[0000-0002-2606-7241]

<sup>1</sup> DTU Technical University of Denmark, Kongens Lyngby, Denmark

<sup>2</sup> IMT School for Advanced Studies Lucca, Italy

<sup>3</sup> University of Aalborg, Denmark

<sup>4</sup> Sant'Anna School for Advanced Studies, Pisa, Italy

**Abstract.** Boolean Networks (BNs) are established models to qualitatively describe biological systems. The analysis of BNs might be infeasible for medium to large BNs due to the state-space explosion problem. We propose a novel reduction technique called *Backward Boolean Equivalence* (BBE), which preserves some properties of interest of BNs. In particular, reduced BNs provide a compact representation by grouping variables that, if initialized equally, are always updated equally. The resulting reduced state space is a subset of the original one, restricted to identical initialization of grouped variables. The corresponding trajectories of the original BN can be exactly restored. We show the effectiveness of BBE by performing a large-scale validation on the whole GINsim BN repository. In selected cases, we show how our method enables analyses that would be otherwise intractable. Our method complements, and can be combined with, other reduction methods found in the literature.

**Keywords:** Boolean Network · State Transition Graph · Attractor Analysis · Exact Reduction · GinSim Repository

## 1 Introduction

Boolean Networks (BNs) are an established method to model biological systems [28]. A BN consists of Boolean variables (also called nodes) which represent the activation status of the components in the model. The variables are commonly depicted as nodes in a network with directed links which represent influences between them. However, a full descriptive mathematical model underlying a BN consists of a set of Boolean functions, the *update functions*, that govern the Boolean values of the variables. Two BNs are displayed on top of Fig. 1. The BN on the left has three variables  $x_1$ ,  $x_2$ , and  $x_3$ , and the BN on

<sup>\*</sup> Partially supported by the DFF project REDUCTO 9040-00224B, the Poul Due Jensen Foundation grant 883901, and the PRIN project SEDUCE 2017TWRCNB.

the right has two variables  $x_{1,2}$  and  $x_3$ . The dynamics (the state space) of a BN is encoded into a *state transition graph* (STG). The bottom part of Fig. 1 displays the STGs of the corresponding BNs. The boxes of the STG represent the BN *states*, i.e. vectors with one Boolean value per BN variable. A directed edge among two STG states represents the evolution of the system from the source state to the target one. The target state is obtained by synchronously applying all the update functions to the activation values of the source state. There exist BN variants with other update schema, e.g. asynchronous non-deterministic [47] or probabilistic [43]. Here we focus on the synchronous case. BNs where variables are *multivalued*, i.e. can take more than two values to express different levels of activation [46], are supported via the use of *booleanization* techniques [18], at the cost, however, of increasing the number of variables.

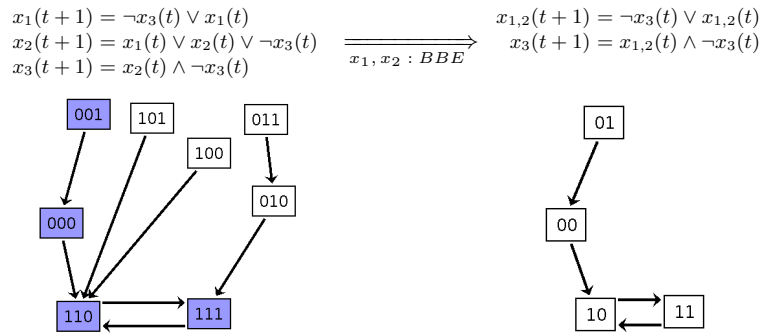


Fig. 1: A BN (top-left), its STG (bottom-left), the BBE-reduced BN (top-right) and its (reduced) STG (bottom-right).

BNs suffer from the state space explosion problem: there are exponentially many STG states with respect to the number of BN variables. This hampers BN analysis in practice, calling for reduction techniques for BNs. There exist manual or semi-automated ones based on domain knowledge. Such empirical reductions have several drawbacks: being semi-automated, they are error-prone, and do not scale. Popular examples are those based on the idea of *variable absorption*, proposed originally in [34,48,41]. The main idea is that certain BN variables can get *absorbed* by the update functions of their target variables by replacing all occurrences of the absorbed variables with their update functions. Other methods automatically remove *leaf* variables (variables with 0 outgoing links) or *frozen* variables (variables that stabilize after some iterations independently of the initial conditions) [39,3]. Several techniques [23,1] focus on reducing the STGs rather than the BN generating them. This requires to construct the original STG, thus still incurring the state space explosion problem.

Our research contributes a novel mathematically grounded method to automatically minimize BNs while exactly preserving behaviors of interest. We present Backward Boolean Equivalence (BBE), which collapses *backward Boolean*

*equivalent* variables. The main intuition is that two BN variables are BBE-equivalent if they maintain equal value in any state reachable from a state wherein they have the same value. In the STG in Fig. 1 (left), we note that for all states where  $x_1$  and  $x_2$  have same value (purple boxes), the update functions do not distinguish them. Notably, BBE is that it can be checked directly on the BN, without requiring to generate the STG. Indeed, as depicted in the middle of Fig. 1,  $x_1$  and  $x_2$  can be shown to be BBE-equivalent by inspecting their update functions: If  $x_1, x_2$  have the same value in a state, i.e.  $x_1(t) = x_2(t)$ , then their update functions will not differentiate them since  $x_2(t+1) = x_1(t) \vee x_2(t) \vee \neg x_3(t) = x_1(t) \vee x_1(t) \vee \neg x_3(t) = x_1(t) \vee \neg x_3(t) = x_1(t+1)$ . We also present an iterative partition refinement algorithm [36] that computes the largest BBE of a BN. Furthermore, given a BBE, we obtain a *BBE-reduced* BN by collapsing all BBE-equivalent variables into one in the reduced BN. In Fig. 1, we collapsed  $x_1, x_2$  into  $x_{1,2}$ . The reduced BN faithfully preserves part of the dynamics of the original BN: it exactly preserves all states and paths of the original STG where BBE-equivalent variables have same activation status. Fig. 1 (right) shows the obtained BBE-reduced BN and its STG. We can see that the purple states of the original STG are preserved in the one of the reduced BN.

We implemented BBE in ERODE [10], a freely available tool for reducing biological systems. We built a toolchain that combines ERODE with several tools for the analysis, visualization and reduction of BNs, allowing us to apply BBE to all BNs from the GINsim repository ([http://ginsim.org/models\\_repository](http://ginsim.org/models_repository)). BBE led to reduction in 61 out of 85 considered models (70%), facilitating STG generation. For two models, we could obtain the STG of the reduced BN while it is not possible to generate the original STG due to its size. We further demonstrate the effectiveness of BBE in three case studies, focusing on their *asymptotic dynamics* by means of *attractors analysis*. Using BBE, we can identify the attractors of large BNs which would be otherwise intractable.

The article is organized as follows: Section 2 provides the basic definitions and the running example based on which we will explain the key concepts. In Section 3, we introduce BBE, present the algorithm for the automatic computation of maximal BBEs, and formalize how the STGs of the original and the reduced BN are related. In Section 4, we apply BBE to BNs from the literature. In Section 5 we discuss related works, while Section 6 concludes the paper.

## 2 Preliminaries

BNs can be represented visually using some graphical representation which, however, might not contain all the information about their dynamics [29]. An example is that of signed interaction (or regulatory) graphs adopted by the tool GinSim [31]. These representations are often paired with a more precise description containing either truth tables [39] or algebraic update functions [45]. In this paper we focus on such precise representation, and in particular on the latter. However, in order to better guide the reader in the case studies, wherein we ma-

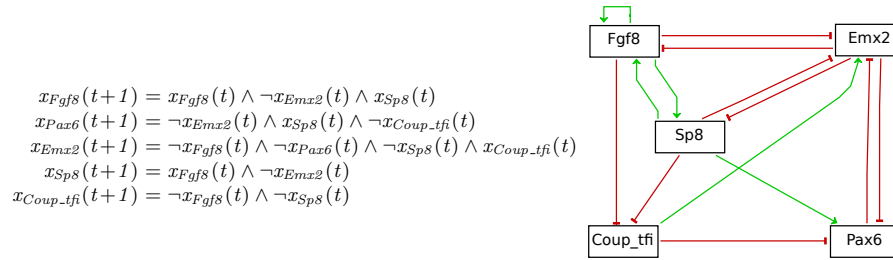


Fig. 2: (Left) the BN of cortical area development from [25]; (Right) its signed interaction graph.

nipulate BNs with a very large number of components, we also introduce signed interaction graphs.

We explain the concepts of current and next sections using the simple BN of Fig. 2 (left) taken from [25]. The model refers to the development of the outer part of the brain: the cerebral cortex. This part of the brain contains different areas with specialised functions. The BN is composed of five variables which represent the gradients that take part in its development: the morphogen  $Fgf8$  and four transcription factors, i.e.,  $Emx2$ ,  $Pax6$ ,  $Coup\_tfi$ ,  $Sp8$ . During development, these genes are expressed in different concentrations across the surface of the cortex forming the different areas.

Fig. 2 (right) displays the signed interaction graph that corresponds to the BN. The green arrows correspond to *activations* whereas the red arrows correspond to *inhibitions*. For example, the green arrow from  $Sp8$  to  $Pax6$  denotes that the former promotes the latter because variable  $x_{Sp8}$  appears (without negation) in the update function of  $x_{Pax6}$ , whereas the red arrow from  $Pax6$  to  $Emx2$  denotes that the former inhibits the latter because the negation of  $x_{Pax6}$  appears in the update function of  $x_{Emx2}$ .

We now give the formal definition of a BN:

**Definition 1.** A BN is a pair  $(X, F)$  where  $X = \{x_1, \dots, x_n\}$  is a set of variables and  $F = \{f_{x_1}, \dots, f_{x_n}\}$  is a set of update functions, with  $f_{x_i} : \mathbb{B}^n \rightarrow \mathbb{B}$  being the update function of variable  $x_i$ .

A BN is often denoted as  $X(t+1) = F(X, t)$ , or just  $X = F(X)$ . In Fig. 2 we have  $X = \{x_{Fgf8}, x_{Pax6}, x_{Emx2}, x_{Sp8}, x_{Coup\_tfi}\}$ .

The *state* of a BN is an evaluation of the variables, denoted with the vector of values  $\mathbf{s} = (s_{x_1}, \dots, s_{x_n}) \in \mathbb{B}^n$ . The variable  $x_i$  has the value  $s_{x_i}$ . When the update functions are applied synchronously, we have synchronous transitions between states, i.e. for  $\mathbf{s}, \mathbf{t} \in \mathbb{B}^n$  we have  $\mathbf{s} \rightarrow \mathbf{t}$  if  $\mathbf{t} = F(\mathbf{s}) = (f_{x_1}(\mathbf{s}), \dots, f_{x_n}(\mathbf{s}))$ .

Suppose that the activation status of the variables  $x_{Fgf8}$ ,  $x_{Emx2}$ ,  $x_{Pax6}$ ,  $x_{Sp8}$ ,  $x_{Coup\_tfi}$  is given by the state  $\mathbf{s} = (1, 0, 1, 1, 1)$ . After applying the update functions, we have  $\mathbf{t} = F(\mathbf{s}) = (0, 0, 0, 0, 0)$ .

The state space of a BN, called *State Transition Graph (STG)*, is the set of all possible states and state transitions.

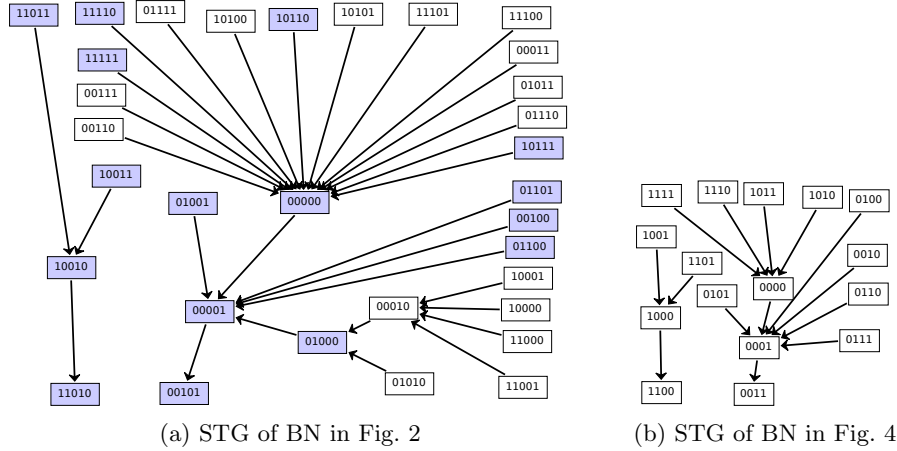


Fig. 3: The STGs of the BN of Fig. 2 and of its BBE-reduction in Fig. 4. We use GINsim’s visual representation, where self-loops are implicit in nodes without outgoing edges.

**Definition 2.** Let  $B = (X, F)$  be a BN. We define the state transition graph of  $B$ , denoted with  $STG(B)$ , as a pair  $(S, T)$  with  $S \subseteq \mathbb{B}^n$  being a set of vertices labelled with the states of  $B$ , and  $T = \{s \rightarrow t \mid s \in S, t = F(s)\}$  a set of directed edges representing the transitions between states of  $B$ .

We often use the notation  $s \rightarrow^+ t$  for the transitive closure of the transition relation. The cardinality of the set of states is  $2^n$ , which illustrates the state space explosion: we have exponentially many states on BN variables. Fig. 3(a) displays the STG of the BN in Fig. 2.

Several BN properties are identified in STGs, e.g. attractors, basins of attraction, and transient trajectories [42]. Attractors are sets of states towards which a system tends to evolve and remain [27]. They are often associated with the interpretation of the underlying system; for example, Kauffman equated attractors with different cell types [20]. Hence, the main reduction methods that have been developed in the literature so far concentrate on how they affect the asymptotic dynamics i.e. the number of attractors and the distribution of their lengths. We define an attractor as follows:

**Definition 3. (Attractor)** Let  $B = (X, F)$  be a BN with  $STG(B) = (S, T)$ . We say that a set of states  $A \subseteq S$  is an attractor iff

1.  $\forall s, s' \in A, s \rightarrow^+ s'$ , and
2.  $\forall s \in A, \forall s' \in S, s \rightarrow^+ s'$  implies  $s' \in A$ .

Attractors are hence just absorbing strongly connected components in the STG. An attractor  $A$  such that  $|A| = 1$  is called a *steady state* (also named *point attractor*). We also denote with  $|A|$  the *length* of attractor  $A$ .

### 3 Backward Boolean Equivalence

Our reduction method is based on the notion of backward equivalence, recast for BNs, which proved to be effective for reducing the dimensionality of ordinary differential equations [9,13] and chemical reaction networks [11,6,8]. Section 3.1 introduces *Backward Boolean Equivalence* (BBE), which is an equivalence relation on the variables of a BN, and use it to obtain a reduced BN. Section 3.2 provides an algorithm which iteratively compute the maximal BBE of a BN. Section 3.3 relates the properties of an original and BBE-reduced BN.

We fix a BN  $B = (X, F)$ , with  $|X| = n$ . We use  $R$  to denote equivalence relations on  $X$  and  $X_R$  for the induced partition.

#### 3.1 Backward Boolean Equivalence and BN Reduction

We first introduce the notion of *constant* state on an equivalence relation  $R$ .

**Definition 4. (Constant State)** A state  $\mathbf{s} \in \mathbb{B}^n$  is constant on  $R$  if and only if  $\forall (x_i, x_j) \in R$  it holds that  $s_{x_i} = s_{x_j}$ .

Consider our running example and an equivalence relation  $R$  given by the partition  $X_R = \{\{x_{Sp8}, x_{Fgf8}\}, \{x_{Pax6}\}, \{x_{Emx2}\}, \{x_{Coup\_tft}\}\}$ . The states constant on  $R$  are colored in purple in Fig. 3. For example, the state  $\mathbf{s} = (1, 0, 1, 1, 1)$  is constant on  $R$  because  $s_{Sp8} = s_{Fgf8}$  (the first and fourth positions of  $\mathbf{s}$ , respectively). On the contrary,  $(1, 0, 1, 0, 1)$  is not constant on  $R$ .

We now define *Backward Boolean Equivalence* (BBE).

**Definition 5. (Backward Boolean Equivalence)** Let  $B = (X, F)$  be a BN,  $X_R$  a partition of the set  $X$  of variables, and  $C \in X_R$  a class of the partition. A partition  $X_R$  is a Backward Boolean Equivalence (BBE) if and only if the following formula is valid:

$$\Phi^{X_R} \equiv \left( \bigwedge_{\substack{C \in X_R \\ x, x' \in C}} (x = x') \right) \longrightarrow \bigwedge_{\substack{C \in X_R \\ x, x' \in C}} (f_x(X) = f_{x'}(X))$$

$\Phi^{X_R}$  says that if for all equivalence classes  $C$  the variables in  $C$  are equal, then the update functions of variables in the same equivalence class stay equal.

In other words,  $R$  is a BBE if and only if for all  $\mathbf{s} \in \mathbb{B}^n$  constant on  $R$  it holds that  $F(\mathbf{s})$  is constant on  $R$ . BBE is a relation where the update functions  $F$  preserve the “constant” property of states. The partition  $X_R = \{\{x_{Sp8}, x_{Fgf8}\}, \{x_{Pax6}\}, \{x_{Emx2}\}, \{x_{Coup\_tft}\}\}$  described above is indeed a BBE. This can be verified on the STG: all purple states (the constant ones) have outgoing transitions only towards purple states.

We now define the notion of BN reduced up to a BBE  $R$ . Each variable in the reduced BN represents one equivalence class in  $R$ . We denote by  $f\{^a/b\}$  the term arising by replacing each occurrence of  $b$  by  $a$  in the function  $f$ .

**Definition 6.** *The reduction of  $B$  up to  $R$ , denoted by  $B/R$ , is the BN  $(X_R, F_R)$  where  $F_R = \{f_{x_C} : C \in X_R\}$ , with  $f_{x_C} = f_{x_k} \{x_{C'} / x_i : \forall C' \in X_R, \forall x_i \in C'\}$  for some  $x_k \in C$ .*

The definition above uses one variable per equivalence class, selects the update function of any variable in such class, and replaces all variables in it with a representative one per equivalence class. Fig. 4 shows the reduction of the cortical area development BN. We selected the update function of  $x_{Sp8}$  as the update function of the class-variable  $x_{\{Fgf8, Sp8\}}$ , and replaced every occurrence of  $x_{Sp8}$  and  $x_{Fgf8}$  with  $x_{\{Fgf8, Sp8\}}$ . The STG of such reduced BN is given in Fig. 3(b).

$$\begin{aligned} x_{\{Fgf8, Sp8\}}(t+1) &= x_{\{Fgf8, Sp8\}}(t) \wedge \neg x_{\{Emx2\}}(t) \\ x_{\{Pax6\}}(t+1) &= \neg x_{\{Emx2\}}(t) \wedge x_{\{Fgf8, Sp8\}}(t) \wedge \neg x_{\{Coup\_tfi\}}(t) \\ x_{\{Emx2\}}(t+1) &= \neg x_{\{Fgf8, Sp8\}}(t) \wedge \neg x_{\{Pax6\}}(t) \wedge \neg x_{\{Fgf8, Sp8\}}(t) \wedge x_{\{Coup\_tfi\}}(t) \\ x_{\{Coup\_tfi\}}(t+1) &= \neg x_{\{Fgf8, Sp8\}}(t) \wedge \neg x_{\{Fgf8, Sp8\}}(t) \end{aligned}$$

Fig. 4: The BBE-reduction of the cortical area development network of Fig. 2.

### 3.2 Computation of the maximal BBE

A crucial aspect of BBE is that it can be checked directly on a BN without requiring the generation of the STG. This is feasible by encoding the logical formula of Definition 5 into a logical SATisfiability problem [2]. A SAT solver has the ability to check the validity of such a logical formula by checking for the unsatisfiability of its negation ( $\text{sat}(\neg\Phi^{X_R})$ ). A partition  $X_R$  is a BBE if and only if  $\text{sat}(\neg\Phi^{X_R})$  returns “unsatisfiable”, otherwise a counterexample (a witness) is returned, consisting of variables assignments that falsify  $\Phi^{X_R}$ . Using counterexamples, it is possible to develop a partition refinement algorithm that computes the largest BBE that refines an initial partition.

The partition refinement algorithm is shown in Algorithm 1. Its input are a BN and an initial partition of its variables  $X$ . A *default* initial partition that leads to the maximal reduction consists of one block only, containing all variables. In general, the modeller may specify a different initial partition if some variables should not be merged together, placing them in different blocks. The output of the algorithm is the largest partition that is a BBE and refines the initial one.

We now explain how the algorithm works for input the cortical area development BN and the initial partition  $X_R = \{\{x_{Fgf8}, x_{Emx2}, x_{Pax6}, x_{Sp8}, x_{Coup\_tfi}\}\}$ .

*Iteration 1.* The algorithm enters the *while* loop, and the solver checks if  $\Phi^{X_R}$  is valid.  $X_R$  is not a BBE, therefore the algorithm enters the second branch of the *if* statement. The solver gives an example satisfying  $\neg\Phi^{X_R}$ :  $s = (s_{x_{Fgf8}}, s_{x_{Pax6}}, s_{x_{Emx2}}, s_{x_{Sp8}}, s_{x_{Coup\_tfi}}) = (0, 0, 0, 0, 0)$ . Since  $t = F(s) = (0, 0, 0, 0, 1)$ , the *for* loop partitions  $G$  into  $X_{R_1} = \{\{x_{Fgf8}, x_{Pax6}, x_{Emx2}, x_{Sp8}\}, \{x_{Coup\_tfi}\}\}$ . The state  $t = (0, 0, 0, 0, 1)$  is now constant on  $X_{R_1}$ .

---

**Algorithm 1:** Compute the maximal BBE that refines the initial partition  $X_R$  for a BN  $(X, F)$

---

**Result:** maximal BBE  $H$  that refines  $X_R$

```

H ← XR;
while true do
  if ΦH is valid then
    | return H ;
  else
    | s ← get a state that satisfy ¬ΦH;
    | H' ← ∅;
    | for C ∈ H do
    |   | C0 = {xi ∈ C : fxi(s) = 0};
    |   | C1 = {xi ∈ C : fxi(s) = 1};
    |   | H' = H' ∪ {C1} ∪ {C0};
    | end
    | H ← H' \ {∅};
  end
end

```

---

*Iteration 2.* The algorithm checks if  $\Phi^{X_{R_1}}$  is valid (i.e. if  $X_{R_1}$  is a BBE).  $X_{R_1}$  is not a BBE. The algorithm gives a counterexample with  $s = (0, 0, 0, 0, 1)$  and  $t = F(s) = (0, 0, 1, 0, 1)$ . The *for* loop refines  $X_{R_1}$  into  $X_{R_2} = \{\{x_{Fgf8}, x_{Pax6}, x_{Sp8}\}, \{x_{Emx2}\}, \{x_{Coup\_tfi}\}\}$ .  $X_{R_2}$  makes  $t = (0, 0, 1, 0, 1)$  constant.

*Iteration 3.* The algorithm checks if  $G_2$  is a BBE. The formula  $\neg\Phi^{X_{R_2}}$  is satisfiable, so  $G_2$  is not a BBE, and the solver provides an example with  $s = (1, 1, 0, 1, 1)$  and  $F(s) = (1, 0, 0, 1, 0)$ . Hence,  $X_{R_2}$  is partitioned into  $X_{R_3} = \{\{x_{Fgf8}, x_{Sp8}\}, \{x_{Pax6}\}, \{x_{Emx2}\}, \{x_{Coup\_tfi}\}\}$ .

*Iteration 4.* The SAT solver proves that  $\Phi^{X_{R_3}}$  is valid.

The number of iterations needed to reach a BBE depends on the counterexamples that the SAT solver provides. As for all partition-refinement algorithms, it can be easily shown that the number of iterations is bound by the number of variables. Each iteration requires to solve a SAT problem which is known to be NP-complete, however we show in Section 4 that we can easily scale to the largest models present in popular BN repositories.

We first show that given an initial partition there exists exactly one *largest* BBE that refines it.<sup>1</sup>

After that, we prove that Algorithm 1 indeed provides the maximal BBE that refines the initial one.

**Theorem 1.** *Let BN = (X, F) and X<sub>R</sub> a partition. There exists a unique maximal BBE H that refines X<sub>R</sub>.*

**Theorem 2.** *Algorithm 1 computes the maximal BBE partition refining X<sub>R</sub>.*

<sup>1</sup> All proofs are given in Appendix A



### 3.3 Relating Dynamics of Original and Reduced BNs

Given a BN  $B$  and a BBE  $R$ ,  $STG(B/R)$  can be seen as the subgraph of  $STG(B)$  composed of all states of  $STG(B)$  that are constant on  $R$  and their transitions. Of course, those states are transformed in  $STG(B/R)$  by “collapsing” BBE-equivalent variables in the state representation. This can be seen by comparing the STG of the our running example (left part of Fig. 3) and of its reduction (right part of Fig. 3). The states (and transitions) of the STG of the reduced BN correspond to the purple states of the original STG.

Let  $B$  be a BN with  $n$  variables,  $S \subseteq \mathbb{B}^n$  be the states of its STG, and  $R$  a BBE for  $B$ . We use  $S_{|R}$  to denote the subset of  $S$  composed by all and only the states constant on  $R$ . With  $STG(B)_{|R}$  we denote the subgraph of  $STG(B)$  containing  $S_{|R}$  and its transitions. Formally  $STG(B)_{|R} = (S_{|R}, T_{|R})$ , where  $T_{|R} = T \cap (S_{|R} \times S_{|R})$ .

The following lemma formalizes a fundamental property of  $STG(B)_{|R}$ , namely that all attractors of  $B$  containing states constant on  $R$  are preserved in  $STG(B)_{|R}$ .

**Lemma 1. (*Constant attractors*)** *Let  $B(X, F)$  be a BN,  $R$  be a BBE, and  $A$  an attractor. If  $A \cap S_{|R} \neq \emptyset$  then  $A \subseteq S_{|R}$ .*

We now define the bijective mapping  $m_R : S_{|R} \leftrightarrow S_R$  induced by a BBE  $R$ , where  $S_R$  are the states of  $STG(B/R)$ , as follows:  $m_R(\mathbf{s}) = (v_{C_1}, \dots, v_{C_{|X/R|}})$  where  $v_{C_j} = s_{x_i}$  for some  $x_i \in C_j$ . In words  $m_R$  bijectively maps each state of  $STG(B)_{|R}$  to their compact representation in  $STG(B/R)$ . Indeed,  $STG(B)_{|R}$  and  $STG(B/R)$  are isomorphic, with  $m_R$  defining their (bijective) relation. We can show this through the following lemma.

**Lemma 2. (*Reduction isomorphism*)** *Let  $B(X, F)$  be a BN and  $R$  be a BBE. Then, it holds*

1. *For all states  $\mathbf{s} \in S_{|R}$  it holds  $F_R(m_R(\mathbf{s})) = m_R(F(\mathbf{s}))$ .*
2. *For all states  $\mathbf{s} \in S_R$  it holds  $F(m_R^{-1}(\mathbf{s})) = m_R^{-1}(F_R(\mathbf{s}))$ .*

The previous Lemma ensures that BBE does not generate spurious trajectories or attractors in the reduced system. We can now state the main result of our approach, namely that the BBE reduction of a BN for a BBE  $R$  exactly preserves all attractors that are constant on  $R$  up to renaming with  $m_R$ .

**Theorem 3. (*Constant attractor preservation*)** *Let  $B(X, F)$  be a BN,  $R$  a BBE, and  $A$  an attractor. If  $A \cap S_{|R} \neq \emptyset$  then  $m_R(A)$  is an attractor for  $B/R$ .*

## 4 Application to BNs from the Literature

We hereby apply BBE to BNs from the GINsim repository. Section 4.1 validates BBE on all models from the repository, while Section 4.2 studies the runtime speedups brought by BBE on attractor-based analysis of selected case studies,

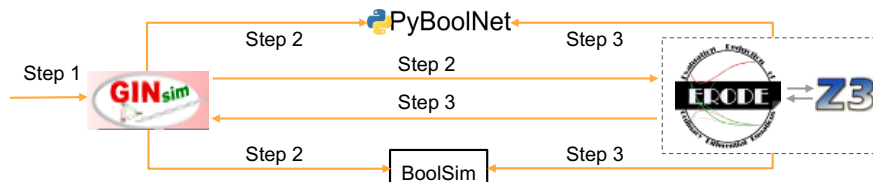


Fig. 5: BBE toolchain. (Step 1) We use GINsim [15] to access its model repository, and (Step 2) export it in the formats of the other tools in the toolchain to perform: STG generation (PyBoolNet [30]), attractor analysis (BoolSim [19]), and BBE reduction (ERODE [10]). (Step 3) We export the reduced models for analysis to PyBoolNet and BoolSim, or to GINsim.

showing cases for which BBE makes the analysis feasible.<sup>2</sup> Section 4.3 compares BBE with the approach based on ODE encoding from [11], showing how such encoding leads to scalability issues and to the loss of reduction power.<sup>3</sup>

The experiments have been made possible by a novel toolchain (Fig. 5) combining tools from the COLOMOTO initiative [33], and the reducer tool ERODE [10] which was extended here to support BBE-reduction. For Algorithm 1 we use the solver Z3 [17] which was already integrated in ERODE.

All experiments were conducted on a common laptop with an Intel Xeon(R) 2.80GHz and 32GB of RAM. We imposed an arbitrary timeout of 24 hours for each task, after which we terminated the analysis. We refer to these cases as *time-out*, while we use *out-of-memory* if a tool terminated with a memory error.

#### 4.1 Large Scale Validation of BBE on BNs

We validate BBE on real-world BNs in terms of the number of BNs that can be reduced and the average reduction ratio.

*Configuration.* We conducted our investigation on the whole GINsim model repository which contains 85 networks: 29 are Boolean, and 56 are multivalued. In multivalued networks (MNs), some variables have more than 2 activation statuses, e.g.  $\{0, 1, 2\}$ . These models are automatically *booleanized* [18,14] by GinSim when exporting in the input formats of the other tools in the tool-chain.

Most of the models in the repository have a specific structure [32] where a few variables are so-called *input variables*. These are variables whose update functions are either a stable function (e.g.  $x(t+1) = 0$ ,  $x(t+1) = 1$ ) or the identity function (e.g.  $x(t+1) = x(t)$ ). These are named ‘input’ because their values are explicitly set by the modeler to perform experiments campaigns. We investigate two reduction scenarios relevant to input variables. In the first one,

<sup>2</sup> These models are further analysed in Appendix C using initial partitions based on information from the original publications, obtaining better reductions.

<sup>3</sup> Appendix D further studies BBE-induced runtime speedups to STG generation on the repository. We display again cases where BBE makes the analysis feasible.

Algorithm 1 starts with initial partitions that lead to the *maximal reduction*, i.e. consisting of one block only. In the second scenario, we provide initial partitions that isolate inputs in singleton blocks. Therefore, we prevent their aggregation with other variables, and obtain reductions independent of the values of the input variables (we recall that BBE requires related variables to be initialized with same activation value). We call this case *input-distinguished (ID) reduction*.

*Results.* By using the maximal reduction setting, we obtained reductions on 61 of the 85 models, while we obtained ID reductions on 38 models. We summarize the reductions obtained for the two settings in Fig. 6, displaying the distribution of the reduction ratios  $r_m = N_m/N$  and  $r_i = N_i/N$ , where  $N$ ,  $N_m$  and  $N_i$  are the number of variables in the original BN, in the maximal BBE-reduction, and in the ID one, respectively.<sup>4</sup> We also provide the average reduction ratios on the models, showing that it does not substantially change across Boolean or multivalued models. No reduction took more than 3 seconds.

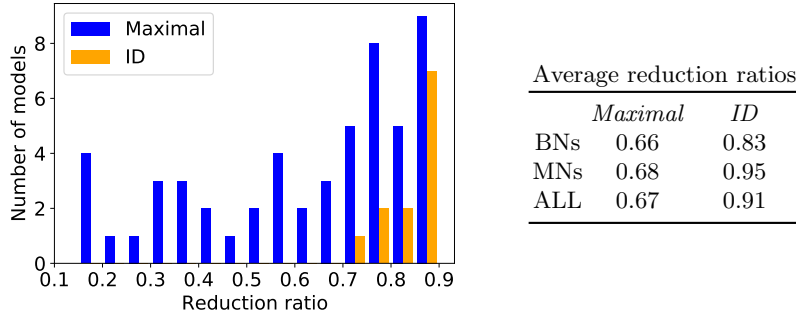


Fig. 6: (Left) Distribution of reduction ratios (reduced variables over original ones) on all models from the GINsim repository using the maximal and ID reduction strategy. Each bar counts the number of models with that reduction ratio, starting from 15% up to 90%, with step 5%. (Right) Average reduction ratios for Boolean, Multivalued and all models.

*Interpretation.* BBE reduced a large number of models (about 72%). In particular, this happened in 24 out of the 29 (83%) Boolean models and in 37 out of 56 (66%) multivalued networks. The average reduction ratio for the maximal and ID strategies are 0.67 and 0.91, respectively. For the former strategy, we get trivial reductions in 22 models wherein only input variables are related. In such trivial cases, the ID strategy does not lead to reduction. In other cases, the target variables of inputs (i.e. variables with incoming edges only from input variables considering the graphical representation of variables) appeared to be

<sup>4</sup> More details can be found in Table 2 of Appendix B.

backward equivalent together with the input variables. This results in reductions with large equivalence classes consisting of input variables and their descendants. These are interesting reductions which get lost using the ID approach, as the input variables get isolated.

## 4.2 Attractor analysis of selected case studies

*Hypothesis.* We now investigate the fate of asymptotic dynamics after BBE-reduction, and test the computational efficiency in terms of time needed for attractor identification in the original and reduced models. We expect that BBE-reduction can be utilized to (i) gain fruitful insights into large BN models and (ii) to reduce the time needed for attractor identification.

*Configuration.* Our analysis focuses on three BNs from the GINsim repository. The first is the Mitogen-Activated Protein Kinases (MAPK) network [26] with 53 variables. The second refers to the survival signaling in large granular lymphocyte leukemia (T-LGL) [52] and contains 60 variables. The third is the merged Boolean model [40] of T-cell and Toll-like receptors (TCR-TLR5) which is the largest BN model in GINsim repository with 128 variables.

*Results.* The results of our analysis are summarized in Table 1 for the original, ID- and maximal-reduced BN. We present the number of variables (*size*) and of Attractors (*Attr.*), the time for attractor identification on the original model (*An. (s)*) and that for reduction plus attractor identification (*Red. + An. (s)*).

	<i>Original model</i>			<i>ID reduction</i>			<i>Maximal reduction</i>		
	<i>Size</i>	<i>Attr.</i>	<i>An.(s)</i>	<i>Size</i>	<i>Attr.</i>	<i>Red.+An.(s)</i>	<i>Size</i>	<i>Attr.</i>	<i>Red.+An.(s)</i>
MAPK Network	53	40	16.50	46	40	15.33	39	17	3.49
T-LGL	60	264	123.43	57	264	86.84	52	6	3.49
TCR-TLR	128	— <i>Time Out</i> —	—	116	— <i>Time Out</i> —	—	95	2	31.29

Table 1: Reduction and attractor analysis on 3 selected case studies.

*Interpretation.* ID reduction preserves all attractors reachable from any combination of activation values for inputs. This is an immediate consequence of 2, Theorem 3 and the fact that number of attractors in the original and the ID reduced BN is the same (see Table 1). Maximal reduction might discard some attractors. We also note that, despite the limited reduction in terms of obtained number of variables, we have important analysis speed-ups, up to two orders of magnitude. Furthermore, the largest model could not be analyzed, while it took just 30 seconds to analyze its maximal reduction identifying 2 attractors.<sup>5</sup>

<sup>5</sup> There might be further attractors of interest in addition to these. In Appendix C we show how BBE could be used by a modeler by imposing ad-hoc initial partitions to preserve more attractors while reducing more than with the ID strategy.

### 4.3 Comparison with ODE-based approach from [11]

As discussed, BBE is based on the backward equivalence notion firstly provided for ordinary differential equations (ODEs), chemical reaction networks, and Markov chains [9,11]. Notably, [11] shows how the notion for ODEs can be applied indirectly to BNs via an *odification* technique [49] to encode BNs as ODEs. Such odification transforms each BN variable into an ODE variable that takes values in the continuous interval [0,1]. The obtained ODEs preserve the attractors of the original BN because the equations of the two models coincide when all variables have value either 0 or 1. However, infinitely more states are added for the cases in which the variables do not have integer value.

*Scalability.* The technique from [11] has been proved able to handle models with millions of variables. Instead, the odification technique is particularly computationally intensive. Due to this, it failed on some models from the GINsim repository, including two from [22], namely *core\_engine\_budding\_yeast\_CC* and *coupled\_budding\_yeast\_CC*, consisting of 39 and 50 variables, respectively. Instead, BBE could be applied in less than a second.

*Reduction power.* Another example is the *TCR-TLR* model from the previous section. In this case, both the ODE-based and BBE techniques succeeded. However, BBE led to better reductions due to the added non-integer states in the ODEs. Intuitively, the ODE-based technique *counts* incoming influences from equivalence classes of nodes, while BBE only checks whether at least one of such influence is present or not. Figure 7 shows an excerpt of the graphical representation of the model by GINsim. We use background colors of nodes to denote BBE equivalence classes (white denotes singleton classes). We see a large equivalence class of magenta species, 3 of which (*IRAK4*, *IRAK1*, and *TAK1*) receive two influences by magenta species, while the others receive only one. This differentiates the species in the ODE-based technique, keeping only the top four in the *magenta* block, while all the others end up in singleton blocks. We compare the original equations of *MyD88* and *IRAK4* which have 1 and 2 incoming influences each.

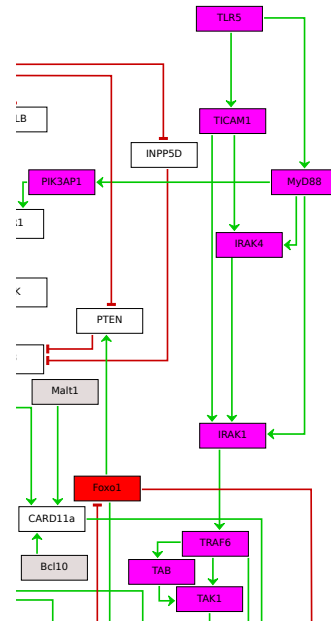


Fig. 7: Excerpt of GINsim’s depict of TCR-TLR.

$$\begin{aligned}
 x_{MyD88}(t + 1) &= x_{TLR5}(t) \\
 x_{IRAK4}(t + 1) &= (\neg x_{MyD88}(t) \wedge x_{TICAM1}(t)) \vee (x_{MyD88}(t))
 \end{aligned}$$

We see that the two variables are BBE because their update functions depend only on the BBE-equivalent variables *TLR5* and *MyD88*, respectively. For *IRAK4*, the three variables in the update function are BBE. Therefore, they have same value allowing us to simplify the update function to just *MyD88*. The ODEs obtained for the 2 variables are, where  $x'_-$  denotes the derivative of  $x_-$ :

$$\begin{aligned}x'_{MyD88} &= x_{TLR5} - x_{MyD88} \\x'_{IRAK4} &= x_{MyD88} + x_{TICAM1} - x_{MyD88} \cdot x_{TICAM1} - x_{IRAK4}\end{aligned}$$

Given that all variables appearing in the equations are backward equivalent, the two equations coincide with the original ones when all variables have values either 0 or 1. However, they differ for non-integer values. For example, in case all variables have value 0.5, we get 0 for the former, and 0.25 for the latter.

## 5 Related Work

BN reduction techniques belong to three families according to their domain of reduction: (i) they reduce at syntactic level (i.e. the BN [34,48,39,3,32,41,51]), (ii) at semantic level (i.e. the STG [23,1]), or (iii) they transform BNs to other formalisms like Petri Nets [16,44] and ordinary differential equations [50] offering formalism-specific reductions. However, (semantic) STG-reduction does not solve the state space explosion whereas the transformation to other formalisms has several drawbacks as shown in Section 4.3.

Syntactic level reduction methods usually perform variable absorption [3,34,48,41] at the BN. BN variables can get absorbed by the update functions of their target variables by replacing all occurrences of the absorbed variables with their update functions. This method was first investigated in [34] wherein update functions are represented as ordinary multivalued decision diagrams. The authors consider multivalued networks with updates being applied asynchronously and iteratively implement absorption. The process, despite preserving steady states in all synchronization schemas [48], might lead to loss of cycle attractors in the synchronous schema. However, absorption of variables might lead to introduction of new attractors in the asynchronous case, i.e., by reducing the number of variables the number of attractors can stay the same or increase (attractors can split or new attractors can appear).

A similar study [48] presents a reduction procedure and proves that it preserves steady states. This procedure includes two steps. The first refers to the deletion of links between variables on their network structure. Deletion of pseudo-influences is feasible by simplifying the Boolean expressions in update functions. The second step of the procedure refers to the absorption of variables like in [34].

The difference between studies [48], [34] is that [48] exploits Boolean algebra instead of multivalued decision diagrams to explain absorption. Moreover, they refer only to Boolean networks, and do not consider any update schema. In studies [34,48,41], self-regulated BN variables (i.e. variables with a self-loop in the graphical representation) can not be selected for absorption. The inability to

absorb self-regulated variables is inherent in the implementation of absorption in contrast to our method where the restrictions are encoded by the user at the initial partition and self-regulated variables can be merged with other variables.

In [41] the authors presented a two step reduction algorithm. The first step includes the absorption of input variables with stable function and the second step the absorption of single mediator variables (variables with one incoming and outgoing edge in the signed interaction graph). The first step of the algorithm in [41] is equally useful and compatible with the first step of [48]. Moreover, if we combine the first steps of [48] and [41], we may achieve interesting reductions which exactly preserve all asymptotic dynamics.

The first steps of [48,41] affect only a BN property called *stability*. Stability is the ability of a BN to end up to the same attractor when starting from slightly different initial conditions. In [3], the authors introduced the decimation procedure -a reduction procedure for synchronous BNs- to discuss how it affects stability. The crucial difference between decimation procedure and BBE-reduction is that the first was invented to study stability whereas the latter was invented to degrade state space explosion. The decimation procedure is summarized by the following four steps: (i) remove from every update functions the inputs that it does not depend on, (ii) find the constant value for variables with no inputs, (iii) propagate the constant values to other update functions and remove this variable from the system, and (iv) if a variable has become constant, repeat from step (i). The study also refers to leaf variables because their presence does not play any role in the asymptotic dynamics of a BN. However, both leaf and fixed-valued variables affect stability. Overall, the decimation procedure exactly preserves the asymptotic dynamics of the original model since it throws out only variables considered as asymptotically irrelevant.

## 6 Conclusion

We introduced an automatic reduction technique for synchronous Boolean Networks which preserves dynamics of interest. The modeller gets a reduced BN based on requirements expressed as an initial partition of variables. The reduced BN can recover a pure part of the original state space and its trajectories established by the reduction isomorphism. Notably, we draw connections between the STG of the original and that of the reduced BN through a rigorous mathematical framework. The dynamics preserved are those wherein collapsed variables have equal values.

We used our reduction technique to speed-up attractor identification. Despite that the length of the preserved attractors is consistent in the reduced model, some of them may get lost. In the future, we plan to study classes of initial partitions that preserve all attractors. We have shown the analysis speed-ups obtained for attractor identification as implemented in the tool BoolSim [24]. In the future we plan to perform a similar analysis on a recent attractor identification approach from [21].

Our method was implemented in ERODE [10], a freely available tool for reducing biological systems. Related *quantitative* techniques offered by ERODE have been recently validated on a large database of biological models [37,38,5]. In the future we plan to extend this analysis considering also BBE. We also plan to investigate whether BBE can be extended in order to be able to compare different models as done for its quantitative counterparts [7,12].

Our method could be combined with most of the existing methods found in literature. Our prototype toolchain consists of several tools from the COLOMOTO interoperability initiative. We aim to incorporate our toolchain into the COLOMOTO Interactive Notebook [35], a unified environment to edit, execute, share, and reproduce analyses of qualitative models of biological networks.

Multivalued BNs, i.e. whose variables can take more than two activation values, are currently supported only via a *booleanization* technique [18,14] that might hamper the interpretability of the reduced model. In future work we plan to generalize BBE to support directly multivalued networks.

## References

1. Bérengruer, D., Chaouiya, C., Monteiro, P.T., Naldi, A., Remy, E., Thieffry, D., Tichit, L.: Dynamical modeling and analysis of large cellular regulatory networks. *Chaos: An Interdisciplinary Journal of Nonlinear Science* **23**(2), 025114 (2013)
2. Biere, A., Biere, A., Heule, M., van Maaren, H., Walsh, T.: *Handbook of Satisfiability: Volume 185 Frontiers in Artificial Intelligence and Applications*. IOS Press, NLD (2009)
3. Bilke, S., Sjunnesson, F.: Stability of the Kauffman model. *Physical Review E* **65**(1), 016129 (2001)
4. Calzone, L., Tournier, L., Fourquet, S., Thieffry, D., Zhivotovsky, B., Barillot, E., Zinovyev, A.: Mathematical modelling of cell-fate decision in response to death receptor engagement. *PLoS Comput Biol* **6**(3), e1000702 (2010)
5. Cardelli, L., Pérez-Verona, I.C., Tribastone, M., Tschaikowski, M., Vandin, A., Waizmann, T.: Exact maximal reduction of stochastic reaction networks by species lumping. *CoRR* **abs/2101.03342** (2021), <https://arxiv.org/abs/2101.03342>
6. Cardelli, L., Tribastone, M., Tschaikowski, M., Vandin, A.: Forward and backward bisimulations for chemical reaction networks. In: 26th International Conference on Concurrency Theory, CONCUR 2015, Madrid, Spain, September 1-4, 2015. pp. 226–239 (2015). <https://doi.org/10.4230/LIPIcs.CONCUR.2015.226>, <https://doi.org/10.4230/LIPIcs.CONCUR.2015.226>
7. Cardelli, L., Tribastone, M., Tschaikowski, M., Vandin, A.: Comparing chemical reaction networks: A categorical and algorithmic perspective. In: Proceedings of the 31st Annual ACM/IEEE Symposium on Logic in Computer Science, LICS '16, New York, NY, USA, July 5-8, 2016. pp. 485–494 (2016). <https://doi.org/10.1145/2933575.2935318>, <https://doi.org/10.1145/2933575.2935318>
8. Cardelli, L., Tribastone, M., Tschaikowski, M., Vandin, A.: Efficient syntax-driven lumping of differential equations. In: Tools and Algorithms for the Construction and Analysis of Systems - 22nd International Conference, TACAS 2016, Held as Part of the European Joint Conferences on Theory and Practice of Software,



- ETAPS 2016, Eindhoven, The Netherlands, April 2-8, 2016, Proceedings. pp. 93–111 (2016). [https://doi.org/10.1007/978-3-662-49674-9\\_6](https://doi.org/10.1007/978-3-662-49674-9_6), [https://doi.org/10.1007/978-3-662-49674-9\\_6](https://doi.org/10.1007/978-3-662-49674-9_6)
9. Cardelli, L., Tribastone, M., Tschaikowski, M., Vandin, A.: Symbolic computation of differential equivalences. In: Proceedings of the 43rd Annual ACM SIGPLAN-SIGACT Symposium on Principles of Programming Languages, POPL 2016, St. Petersburg, FL, USA, January 20 - 22, 2016. pp. 137–150 (2016). <https://doi.org/10.1145/2837614.2837649>, <https://doi.org/10.1145/2837614.2837649>
  10. Cardelli, L., Tribastone, M., Tschaikowski, M., Vandin, A.: Erode: a tool for the evaluation and reduction of ordinary differential equations. In: International Conference on Tools and Algorithms for the Construction and Analysis of Systems. pp. 310–328. Springer (2017)
  11. Cardelli, L., Tribastone, M., Tschaikowski, M., Vandin, A.: Maximal aggregation of polynomial dynamical systems. Proceedings of the National Academy of Sciences **114**(38), 10029–10034 (2017)
  12. Cardelli, L., Tribastone, M., Tschaikowski, M., Vandin, A.: Comparing chemical reaction networks: A categorical and algorithmic perspective. Theor. Comput. Sci. **765**, 47–66 (2019). <https://doi.org/10.1016/j.tcs.2017.12.018>, <https://doi.org/10.1016/j.tcs.2017.12.018>
  13. Cardelli, L., Tribastone, M., Tschaikowski, M., Vandin, A.: Symbolic computation of differential equivalences. Theor. Comput. Sci. **777**, 132–154 (2019). <https://doi.org/10.1016/j.tcs.2019.03.018>, <https://doi.org/10.1016/j.tcs.2019.03.018>
  14. Chaouiya, C., Bérenguier, D., Keating, S.M., Naldi, A., Van Iersel, M.P., Rodriguez, N., Dräger, A., Büchel, F., Cokelaer, T., Kowal, B., et al.: SBML qualitative models: a model representation format and infrastructure to foster interactions between qualitative modelling formalisms and tools. BMC systems biology **7**(1), 1–15 (2013)
  15. Chaouiya, C., Naldi, A., Thieffry, D.: Logical modelling of gene regulatory networks with ginsim. In: Bacterial Molecular Networks, pp. 463–479. Springer (2012)
  16. Chaouiya, C., Remy, E., Thieffry, D.: Petri net modelling of biological regulatory networks. Journal of Discrete Algorithms **6**(2), 165–177 (2008)
  17. De Moura, L., Bjørner, N.: Z3: An efficient smt solver. In: International conference on Tools and Algorithms for the Construction and Analysis of Systems. pp. 337–340. Springer (2008)
  18. Delaplace, F., Ivanov, S.: Bisimilar booleanization of multivalued networks. BioSystems p. 104205 (2020)
  19. Di Cara, A., Garg, A., De Micheli, G., Xenarios, I., Mendoza, L.: Dynamic simulation of regulatory networks using squad. BMC bioinformatics **8**(1), 462 (2007)
  20. Drossel, B.: Random boolean networks. Reviews of nonlinear dynamics and complexity **1**, 69–110 (2008)
  21. Dubrova, E., Teslenko, M.: A sat-based algorithm for finding attractors in synchronous boolean networks. IEEE/ACM transactions on computational biology and bioinformatics **8**(5), 1393–1399 (2011)
  22. Fauré, A., Naldi, A., Lopez, F., Chaouiya, C., Ciliberto, A., Thieffry, D.: Modular logical modelling of the budding yeast cell cycle. Molecular bioSystems **5**, 1787–96 (2009 Dec 2009)
  23. Figueiredo, D.: Relating bisimulations with attractors in boolean network models. In: International Conference on Algorithms for Computational Biology. pp. 17–25. Springer (2016)

24. Garg, A., Di Cara, A., Xenarios, I., Mendoza, L., De Micheli, G.: Synchronous versus asynchronous modeling of gene regulatory networks. *Bioinformatics* **24**(17), 1917–1925 (07 2008). <https://doi.org/10.1093/bioinformatics/btn336>, <https://doi.org/10.1093/bioinformatics/btn336>
25. Giacomantonio, C.E., Goodhill, G.J.: A boolean model of the gene regulatory network underlying mammalian cortical area development. *PLOS Computational Biology* **6**(9), 1–13 (09 2010). <https://doi.org/10.1371/journal.pcbi.1000936>, <https://doi.org/10.1371/journal.pcbi.1000936>
26. Grieco, L., Calzone, L., Bernard-Pierrot, I., Radvanyi, F., Kahn-Perles, B., Thieffry, D.: Integrative modelling of the influence of mapk network on cancer cell fate decision. *PLoS Comput Biol* **9**(10), e1003286 (2013)
27. Hopfensitz, M., Müssel, C., Maucher, M., Kestler, H.A.: Attractors in boolean networks: a tutorial. *Computational Statistics* **28**(1), 19–36 (2013)
28. Kauffman, S.: Metabolic stability and epigenesis in randomly constructed genetic nets. *Journal of Theoretical Biology* **22**(3), 437 – 467 (1969)
29. Klamt, S., Haus, U.U., Theis, F.: Hypergraphs and cellular networks. *PLoS computational biology* **5**(5) (2009)
30. Klarner, H., Streck, A., Siebert, H.: Pyboolnet: a python package for the generation, analysis and visualization of boolean networks. *Bioinformatics* **33**(5), 770–772 (2017)
31. Naldi, A., Berenguier, D., Fauré, A., Lopez, F., Thieffry, D., Chaouiya, C.: Logical modelling of regulatory networks with ginsim 2.3. *Biosystems* **97**(2), 134–139 (2009)
32. Naldi, A., Monteiro, P.T., Chaouiya, C.: Efficient handling of large signalling-regulatory networks by focusing on their core control. In: *International Conference on Computational Methods in Systems Biology*. pp. 288–306. Springer (2012)
33. Naldi, A., Monteiro, P.T., Müssel, C., for Logical Models, C., Tools, Kestler, H.A., Thieffry, D., Xenarios, I., Saez-Rodriguez, J., Helikar, T., Chaouiya, C.: Cooperative development of logical modelling standards and tools with colomoto. *Bioinformatics* **31**(7), 1154–1159 (2015)
34. Naldi, A., Remy, E., Thieffry, D., Chaouiya, C.: Dynamically consistent reduction of logical regulatory graphs. *Theoretical Computer Science* **412**(21), 2207–2218 (2011)
35. Naldi, A., Hernandez, C., Levy, N., Stoll, G., Monteiro, P.T., Chaouiya, C., Helikar, T., Zinovyev, A., Calzone, L., Cohen-Boulakia, S., Thieffry, D., Paulevé, L.: The colomoto interactive notebook: Accessible and reproducible computational analyses for qualitative biological networks. *Frontiers in Physiology* **9**, 680 (2018). <https://doi.org/10.3389/fphys.2018.00680>, <https://www.frontiersin.org/article/10.3389/fphys.2018.00680>
36. Paige, R., Tarjan, R.E.: Three partition refinement algorithms. *SIAM Journal on Computing* **16**(6), 973–989 (1987)
37. Pérez-Verona, I.C., Tribastone, M., Vandin, A.: A large-scale assessment of exact model reduction in the biomodels repository. In: *Computational Methods in Systems Biology - 17th International Conference, CMSB 2019, Trieste, Italy, September 18-20, 2019, Proceedings*. pp. 248–265 (2019). [https://doi.org/10.1007/978-3-030-31304-3\\_13](https://doi.org/10.1007/978-3-030-31304-3_13), [https://doi.org/10.1007/978-3-030-31304-3\\_13](https://doi.org/10.1007/978-3-030-31304-3_13)
38. Pérez-Verona, I.C., Tribastone, M., Vandin, A.: A large-scale assessment of exact model reduction in the biomodels repository. *Theoretical Computer Science* (2021)
39. Richardson, K.A.: Simplifying boolean networks. *Advances in Complex Systems* **8**(04), 365–381 (2005)

40. Rodríguez-Jorge, O., Kempis-Calanis, L.A., Abou-Jaoudé, W., Gutiérrez-Reyna, D.Y., Hernandez, C., Ramirez-Pliego, O., Thomas-Chollier, M., Spicuglia, S., Santana, M.A., Thieffry, D.: Cooperation between t cell receptor and toll-like receptor 5 signaling for cd4+ t cell activation. *Science signaling* **12**(577) (2019)
41. Saadatpour, A., Albert, R., Reluga, T.C.: A reduction method for boolean network models proven to conserve attractors. *SIAM Journal on Applied Dynamical Systems* **12**(4), 1997–2011 (2013)
42. Schwab, J.D., Kühlwein, S.D., Ikonomi, N., Kühl, M., Kestler, H.A.: Concepts in boolean network modeling: What do they all mean? *Computational and Structural Biotechnology Journal* **18**, 571 – 582 (2020). <https://doi.org/https://doi.org/10.1016/j.csbj.2020.03.001>, <http://www.sciencedirect.com/science/article/pii/S200103701930460X>
43. Shmulevich, I., Dougherty, E.R., Kim, S., Zhang, W.: Probabilistic boolean networks: a rule-based uncertainty model for gene regulatory networks. *Bioinformatics* **18**(2), 261–274 (2002)
44. Stegles, L.J., Banks, R., Shaw, O., Wipat, A.: Qualitatively modelling and analysing genetic regulatory networks: a petri net approach. *Bioinformatics* **23**(3), 336–343 (2007)
45. Su, C., Pang, J.: Sequential control of boolean networks with temporary and permanent perturbations. *arXiv preprint arXiv:2004.07184* (2020)
46. Thomas, R.: Regulatory networks seen as asynchronous automata: a logical description. *Journal of theoretical biology* **153**(1), 1–23 (1991)
47. Thomas, R.: Kinetic logic: a Boolean approach to the analysis of complex regulatory systems: proceedings of the EMBO course “formal analysis of genetic regulation”, held in Brussels, September 6–16, 1977, vol. 29. Springer Science & Business Media (2013)
48. Veliz-Cuba, A.: Reduction of boolean network models. *Journal of theoretical biology* **289**, 167–172 (2011)
49. Wittmann, D.M., Krumsiek, J., Saez-Rodriguez, J., Lauffenburger, D.A., Klamt, S., Theis, F.J.: Transforming boolean models to continuous models: methodology and application to T-cell receptor signaling. *BMC Systems Biology* **3**(1), 98 (2009). <https://doi.org/10.1186/1752-0509-3-98>
50. Wittmann, D.M., Krumsiek, J., Saez-Rodriguez, J., Lauffenburger, D.A., Klamt, S., Theis, F.J.: Transforming boolean models to continuous models: methodology and application to t-cell receptor signaling. *BMC systems biology* **3**(1), 98 (2009)
51. Zañudo, J.G.T., Albert, R.: An effective network reduction approach to find the dynamical repertoire of discrete dynamic networks. *Chaos: An Interdisciplinary Journal of Nonlinear Science* **23**(2), 025111 (2013). <https://doi.org/10.1063/1.4809777>, <https://doi.org/10.1063/1.4809777>
52. Zhang, R., Shah, M.V., Yang, J., Nyland, S.B., Liu, X., Yun, J.K., Albert, R., Loughran, T.P.: Network model of survival signaling in large granular lymphocyte leukemia. *Proceedings of the National Academy of Sciences* **105**(42), 16308–16313 (2008)

## A Proofs

*Proof (Proof of Theorem 1).* Let  $X_{R_1}, X_{R_2}$  be two BBE partitions that refine some other partition  $X_I$  that is not necessarily a BBE. We start by noting that  $R = (R_1 \cup R_2)^* \subseteq I$  because  $R_1, R_2 \subseteq I$ , where asterisk denotes the transitive closure, while  $R_1, R_2$  and  $I$  are equivalence relations underlying  $X_{R_1}, X_{R_2}$  and  $X_I$ , respectively. Hence,  $X_R$  is a refinement of  $X_I$ . We next show that  $X_R$  is a BBE partition. To this end, fix some  $\mathbf{s} \in \mathbb{B}^n$  that is constant on  $R$ . Since  $R_i \subseteq R$ , this implies that  $\mathbf{s}$  is constant on  $R_i$  which, in virtue of  $X_{R_i}$  being a BBE, implies that  $F(\mathbf{s}) \in \mathbb{B}^n$  is constant on  $R_i$ . This implies that  $F(\mathbf{s}) \in \mathbb{B}^n$  is constant on  $R = (R_1 \cup R_2)^*$ , thus showing that  $X_R$  is indeed a BBE partition. The overall claim follows by noting that the finiteness of  $X$  implies that there are finitely many BBE partitions  $X_{R_i}$  that refine any given partition  $X_I$  of  $X$ .

*Proof (Proof of Theorem 2).* Assume that  $G'$  denotes the coarsest BBE partition that refines some given partition  $G$ . Set  $H_0 := G$  and define for all  $k \geq 0$

$$H_{k+1} := (\{C_0 \mid C \in H_k\} \cup \{C_1 \mid C \in H_k\}) \setminus \{\emptyset\},$$

where  $C_0$  and  $C_1$  are as in Algorithm 1. Then, a proof by induction over  $k \geq 1$  shows that (a)  $G'$  is a refinement of  $H_k$  and (b)  $H_k$  is a refinement of  $H_{k-1}$ , for all  $k \geq 1$ . Since  $G'$  is a refinement of any  $H_k$ , it holds that  $G' = H_k$  if  $H_k$  is a BBE partition. Since  $X$  is finite, b) allows us to fix the smallest  $k \geq 1$  such that  $H_k = H_{k-1}$ . This, in turn, implies that  $H_{k-1}$  is a BBE.

*Proof (Proof of Lemma 1).* The fact that  $A \cap S_{|R} \neq \emptyset$  implies that there is at least one state  $\mathbf{s} \in A$  that is constant on  $R$ , i.e.,  $\mathbf{s} \in A \cap S_{|R}$ . For any such state  $\mathbf{s}$ , by the properties of BBE we have that any state  $\mathbf{t}$  such that  $\mathbf{s} \rightarrow^+ \mathbf{t}$  is also constant on  $R$ . Actually, it is trivial to show that  $A = \{\mathbf{t} \mid \mathbf{s} \rightarrow^+ \mathbf{t}\}$ . It immediately follows that  $A \subseteq S_{|R}$ .

*Proof (Proof of Lemma 2).* Follows readily from the definition of a BBE and  $m_R$ .

*Proof (Proof of Theorem 3).* The theorem trivially follows from Lemmas 1 and 2.

## B Table of large-scale validation

We provide the table referenced in the Section 4.1 on large-scale validation of BBE. The table contains the results of BBE reduction on all the models from the GINsim repository. The first column contains the model identifier (MI). The second column contains the url to download the model and the third column displays the number of variables in the original BN. In the case of multivalued networks, the column contains the number of variables after booleanization. We denote with  $N_m, N_i$  the number of variables of the maximal and the ID reduced BN in the fifth and sixth column respectively. Note that when a BN has no input variables  $N_i$  and  $N_m$  coincide. The last two columns display the reduction ratios  $r_i = N_i/N, r_m = N_m/N$  where  $N$  is the number of variables in the original BN.

<i>MI</i>	<i>GINsim repository URI</i>	<i>N</i>	<i>N<sub>i</sub></i>	<i>N<sub>m</sub></i>	<i>r<sub>i</sub></i>	<i>r<sub>m</sub></i>
B1	<a href="http://ginsim.org/node/225">http://ginsim.org/node/225</a>	128	107	95	0.836	0.742
B2	<a href="http://ginsim.org/node/225">http://ginsim.org/node/225</a>	110	103	91	0.936	0.827
B3	<a href="http://ginsim.org/node/87">http://ginsim.org/node/87</a>	60	57	52	0.95	0.867
B4	<a href="http://ginsim.org/node/173">http://ginsim.org/node/173</a>	53	46	39	0.868	0.736
B5	<a href="http://ginsim.org/node/225">http://ginsim.org/node/225</a>	42	37	29	0.881	0.690
B6	<a href="http://ginsim.org/node/78">http://ginsim.org/node/78</a>	40	31	29	0.775	0.725
B7	<a href="http://ginsim.org/node/227">http://ginsim.org/node/227</a>	33	27	25	0.818	0.758
B8	<a href="http://ginsim.org/node/191">http://ginsim.org/node/191</a>	32	32	31	1	0.969
B9	<a href="http://ginsim.org/node/227">http://ginsim.org/node/227</a>	28	25	20	0.893	0.714
B10	<a href="http://ginsim.org/node/97">http://ginsim.org/node/97</a>	26	23	4	0.885	0.154
B11	<a href="http://ginsim.org/node/144">http://ginsim.org/node/144</a>	24	23	9	0.958	0.375
B12	<a href="http://ginsim.org/node/126">http://ginsim.org/node/126</a>	24	21	4	0.875	0.167
B13	<a href="http://ginsim.org/node/102">http://ginsim.org/node/102</a>	23	22	8	0.957	0.348
B14	<a href="http://ginsim.org/node/39">http://ginsim.org/node/39</a>	20	15	13	0.75	0.65
B15	<a href="http://ginsim.org/node/160">http://ginsim.org/node/160</a>	18	18	8	1	0.444
B16	<a href="http://ginsim.org/node/35">http://ginsim.org/node/35</a>	18	17			0.944
B17	<a href="http://ginsim.org/node/31">http://ginsim.org/node/31</a>	14	14	12	1	0.857
B18	<a href="http://ginsim.org/node/152">http://ginsim.org/node/152</a>	11	10	9	0.909	0.818
B19	<a href="http://ginsim.org/node/37">http://ginsim.org/node/37</a>	10	9	9	0.9	0.9
B20	<a href="http://ginsim.org/node/69">http://ginsim.org/node/69</a>	10	8	8	0.8	0.8
B21	<a href="http://ginsim.org/model/C_crescentus">http://ginsim.org/model/C_crescentus</a>	9	7			0.778
B22	<a href="http://ginsim.org/node/21">http://ginsim.org/node/21</a>	9	7			0.778
B23	<a href="http://ginsim.org/node/214">http://ginsim.org/node/214</a>	6	2			0.333
B24	<a href="http://ginsim.org/model/C_crescentus">http://ginsim.org/model/C_crescentus</a>	5	1			0.2
M1	<a href="http://ginsim.org/model/tcell-checkpoint-inhibitors-tcla4-pd1">http://ginsim.org/model/tcell-checkpoint-inhibitors-tcla4-pd1</a>	218	201	136	0.922	0.623
M2	<a href="http://ginsim.org/node/229">http://ginsim.org/node/229</a>	133	126	122	0.947	0.917
M3	<a href="http://ginsim.org/node/178">http://ginsim.org/node/178</a>	107	93	59	0.869	0.551
M4	<a href="http://ginsim.org/node/185">http://ginsim.org/node/185</a>	103	97	52	0.941	0.505
M5	<a href="http://ginsim.org/model/SP">http://ginsim.org/model/SP</a>	102	16			0.157
M6	<a href="http://ginsim.org/node/194">http://ginsim.org/node/194</a>	83	79			0.951
M7	<a href="http://ginsim.org/node/79">http://ginsim.org/node/79</a>	71	69	42	0.972	0.592
M8	<a href="http://ginsim.org/node/234">http://ginsim.org/node/234</a>	61	60	58	0.983	0.95
M9	<a href="http://ginsim.org/model/drosophila_mesoderm">http://ginsim.org/model/drosophila_mesoderm</a>	57	57	11	1	0.192
M10	<a href="http://ginsim.org/node/69">http://ginsim.org/node/69</a>	56	56	50	1	0.893
M11	<a href="http://ginsim.org/model/EMT_Selvaggio_etal">http://ginsim.org/model/EMT_Selvaggio_etal</a>	56	56	43	1	0.768
M12	<a href="http://ginsim.org/node/229">http://ginsim.org/node/229</a>	53	51	50	0.962	0.943
M13	<a href="http://ginsim.org/node/21">http://ginsim.org/node/21</a>	50	49	41	0.98	0.82
M14	<a href="http://ginsim.org/node/180">http://ginsim.org/node/180</a>	48	35			0.729
M15	<a href="http://ginsim.org/node/25">http://ginsim.org/node/25</a>	39	37	31	0.948	0.794
M16	<a href="http://ginsim.org/model/sex_determination_chicken">http://ginsim.org/model/sex_determination_chicken</a>	37	37	14	1	0.378
M17	<a href="http://ginsim.org/node/79">http://ginsim.org/node/79</a>	36	35	21	0.972	0.583
M18	<a href="http://ginsim.org/node/188">http://ginsim.org/node/188</a>	35	34	28	0.971	0.8
M19	<a href="http://ginsim.org/node/216">http://ginsim.org/node/216</a>	34	34	33	1	0.971
M20	<a href="http://ginsim.org/node/96">http://ginsim.org/node/96</a>	34	32	15	0.941	0.441
M21	<a href="http://ginsim.org/node/183">http://ginsim.org/node/183</a>	30	30	14	1	0.467
M22	<a href="http://ginsim.org/model/eggshell_patterning">http://ginsim.org/model/eggshell_patterning</a>	24	23	12	0.958	0.5
M23	<a href="http://ginsim.org/node/41">http://ginsim.org/node/41</a>	21	21	18	1	0.857
M24	<a href="http://ginsim.org/model/sex_determination_mammals">http://ginsim.org/model/sex_determination_mammals</a>	19	19	12	1	0.632
M25	<a href="http://ginsim.org/node/109">http://ginsim.org/node/109</a>	19	19	7	1	0.368
M26	<a href="http://ginsim.org/model/SP">http://ginsim.org/model/SP</a>	19	18	17	0.947	0.895
M27	<a href="http://ginsim.org/node/89">http://ginsim.org/node/89</a>	18	18	10	1	0.556
M28	<a href="http://ginsim.org/node/29">http://ginsim.org/node/29</a>	16	16	13	1	0.812
M29	<a href="http://ginsim.org/model/sex_determination_chicken">http://ginsim.org/model/sex_determination_chicken</a>	15	15	13	1	0.866
M30	<a href="http://ginsim.org/node/194">http://ginsim.org/node/194</a>	14	14	13	1	0.928
M31	<a href="http://ginsim.org/node/26">http://ginsim.org/node/26</a>	12	12	8	1	0.667
M32	<a href="http://ginsim.org/node/115">http://ginsim.org/node/115</a>	16	16	5	1	0.3125
M33	<a href="http://ginsim.org/node/220">http://ginsim.org/node/220</a>	10	10	8	1	0.8
M34	<a href="http://ginsim.org/model/eggshell_patterning">http://ginsim.org/model/eggshell_patterning</a>	8	8	2	1	0.25
M35	<a href="http://ginsim.org/node/82">http://ginsim.org/node/82</a>	7	7	6	1	0.857
M36	<a href="http://ginsim.org/node/82">http://ginsim.org/node/82</a>	7	7	6	1	0.857
M37	<a href="http://ginsim.org/node/50">http://ginsim.org/node/50</a>	6	6	5	1	0.833

Table 2: Application of BBE to BNs from the GINsim model repository.

## C Refined initial partitions for the selected case studies

In Section 4.2, we studied how BBE affects attractor analysis of three selected case studies. It is remarkable that attractor identification was infeasible for the largest TCR-TLR5 BN, whereas we identified its attractors in 30 seconds in its maximal reduction. However, the attractors identified may not be all the attractors of interest for the BN. Our crucial hypothesis is that one can specify alternative initial partitions that preserve more or discard some irrelevant attractors. We also expect that the reduction ratio of these alternative initial partitions lies between that of the ID and that of the maximal reduction ( $r_m$ ,  $r_i$ ).

*Configuration* In Sections C.1 , C.2 and C.3 , we provide a detailed description of the initial partitions that lead to the *refined reduced models*.

*Results* The results of the refined MAPK, the refined merged TCR-TLR, and the refined T-LGL reduced models are summarized in the following Table 3 . We present the number of variables (*Size*), the number of *Attractors*, and the time needed for reduction (*Reduction (s)*) and attractor identification (*Analysis (s)*).

<i>Model</i>	<i>Original model</i>			<i>Refined Reduced model</i>			
	<i>Size</i>	<i>Attractors</i>	<i>Analysis (s)</i>	<i>Reduction (s)</i>	<i>Size</i>	<i>Attractors</i>	<i>Analysis (s)</i>
MAPK Network	53	40	16.501	1.202	42	40	12.115
T-LGL	60	264	123.431	1,816	56	120	55.049
TCR-TLR merged	128	— <i>Time Out</i> —		2.096	98	8	9349.577

Table 3: The results of 3 case studies for the original and the refined reduced BNs

The refined reduced MAPK network consists of 42 variables but preserves all attractors in the original model. Notably, the reduced model has 80% the size of the original. The refined reduced T-LGL results from the original after specifying two input variables in the same block of the initial partition. The merging of these two input variables is an immediate result of [52] and discards 144 attractors which are irrelevant for their analysis. Last but not least, the refined reduced TCR-TLR merged has 98 variables and 8 attractors-more than the maximal reduction of Table 1 . Note again that the attractor identification in the original BN is intractable.

*Interpretation* Overall, Table 3 illustrates the possibility of analyzing large BNs by defining alternative initial partitions than the two considered in Section 4.1. Alternative reductions may provide fruitful insights and identify crucial properties of the underlying system. The size of the refined reduced model lies between the size of the input-distinguished and the maximal reduced model in all three models.

The initialization of Algorithm 1 provides also a framework to specify desires and limitations. Desires refer to the preserved properties with respect to the original model whereas limitations refer to variable perturbation. If such a variable get merged then its perturbation will indicate subsequent perturbation to all the variables that belong to its class. Consequently, variables that are amenable to perturbation, should be kept in singleton blocks of the initial partition. To this end, we can construct empirical initial partitions that (i) preserve attractors, (ii) discard some of them, or (iii) isolate in singleton blocks variables which are amenable to perturbation.

### C.1 T Cell and Toll-like Receptor (TCR-TLR) merged signalling BN

In this Section, we exploit the results from the maximal and the ID reduction to obtain two refined reduced BNs of the TCR-TLR merged BN. This BN refers to the T cell receptors and their responsibility for the activation of T cell ([40], Fig. 9). The authors generated logical models for the TCR and the TLR5 signalling pathways, and merged them by considering their cross interactions. The original model contains 128 variables, fact that renders its analysis intractable. In order to experimentally validate the correctness of their new merged BN, they considered asynchronous update schema and performed reduction with absorption [34]. Absorption does not guarantee preservation of all asymptotic dynamics. It has been proven [48,34,41] that preserves only steady states and may cause spurious cyclic attractors when applied to asynchronous dynamics. When applied to synchronous dynamics, this method may also degenerate cyclic attractors. BBE-reduction maintain the lengths of the preserved attractors according to Theorem 3.

*ID reduction* The application of ID reduction to the merged model resulted in 10 equivalence classes displayed in Fig. 8 . We also display them in Fig. 9 with different colors for each class: Backward equivalent variables are represented with colored boxes, and colored boxes that belong to the same equivalence class have the same background. Variables in white background belong to singleton classes. The ID reduced BN is still huge (116 variables) and the attractor identification is intractable.

$$\begin{array}{ll}
 \{IRAK4, PIK3AP1\} & \{GRAP2, MAP4K1\} \\
 \{TICAM1, MyD88\} & \{MKNK1, RPS6KA5\} \\
 \{Foxo1, BAD, GSK3B, CDKN1A\} & \{MAPKAPK2, mTOR\} \\
 \{MAP2K3, MAP2K7\} & \{Camk2, Camk4\} \\
 \{Cyc1, CTNNB1\} & \{DAG, IP3\}
 \end{array}$$

Fig. 8: The equivalence classes of the input-distinguished reduction

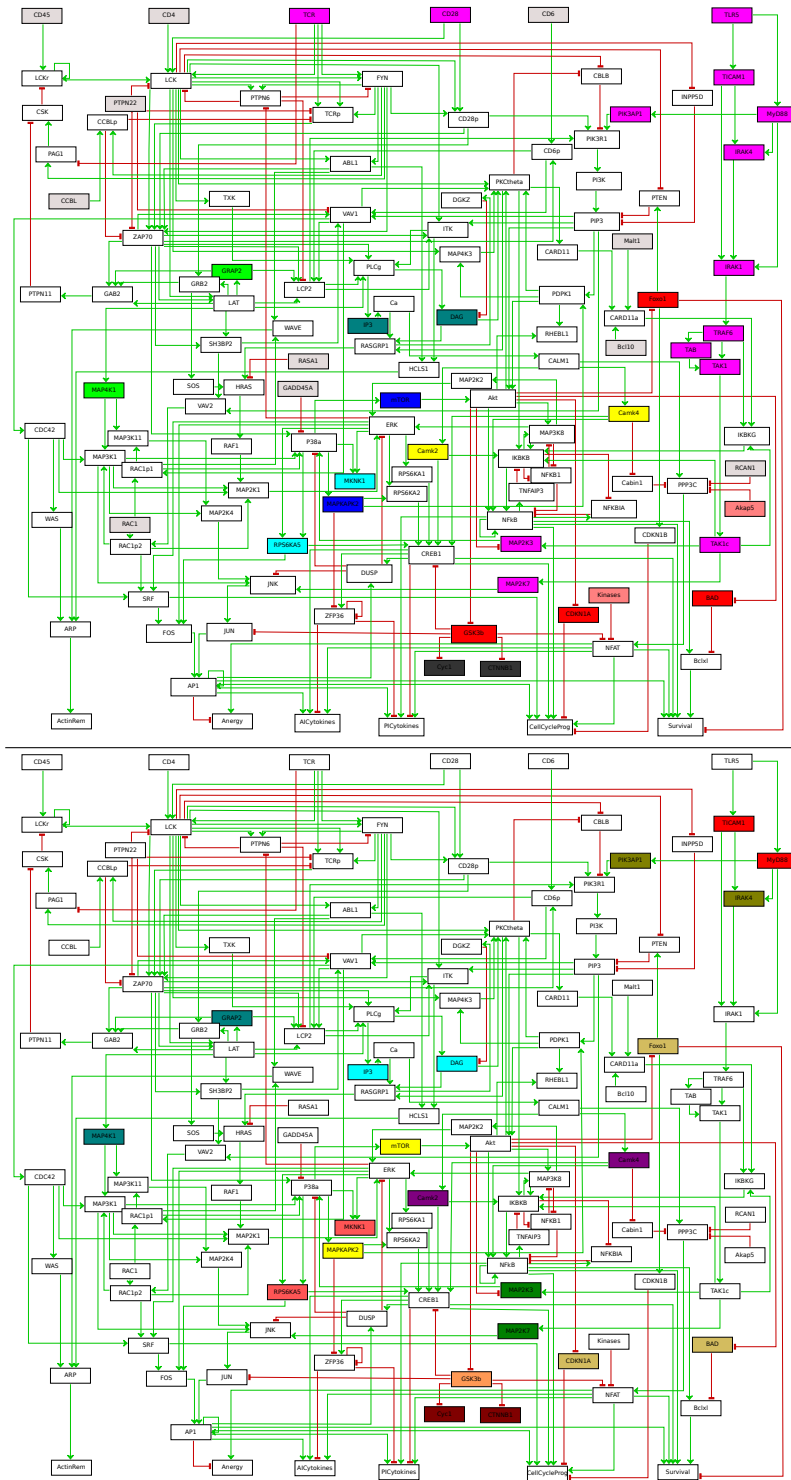


Fig. 9: Up: The TCR-TLR merged BN with input-distinguishing BBE-variables having the same background color. Bottom: The TCR-TLR merged BN with maximal-reduction BBE-variables having the same background color. Variables with white background belong to singleton classes.



*Maximal reduction* However, the maximal reduced BN contains 95 variables and the attractor identification is feasible in 29.336 seconds. Fig. 9 displays the following BBE-equivalence classes with different colors:

*{ <i>CD45, CD4, CD6, CCBL,</i> <i>PTPN22, Malt1, Bcl10, RCAN1,</i> <i>RAC1, RASA1, GDD45A}</i> { <i>MAPKAPK2, mTOR</i> } { <i>MKNK1, RPS6KA5</i> } { <i>DAG, IP3</i> } { <i>Camk2, Camk4</i> }	***{ <i>TCR, CD28, TLR5, TICAM1, PIK3AP1,</i> <i>MyD88, IRAK1 TRAF6, TAB, TAK1,</i> <i>TAK1c, IRAK4, MAP2K3, MAP2K7</i> } ** { <i>Kinases, Akap5</i> } { <i>Foxo1, BAD, GSK3B, CDKN1A</i> } { <i>GRAP2, MAP4K1</i> } { <i>Cyc1, CTNNB1</i> }
---	--

Fig. 10: The equivalence classes of the maximal reduction

The maximal reduction splits input variables into 3 classes: The first class (\*) in Fig. 10) contains all variables with stable update function which equals to *true*. The second class (\*\*) contains all variables with stable update functions that equals to *false*. The third class (\*\*\*) contains all variables with identity update function (*TCR, CD28, TLR5*) and all variables BBE-equivalent variables with them.

*Refined Reduction* We now consider two alternative initial partitions, initialize Algorithm 1 with them, and gain deeper insights in the underlying model. The first initial partition is constructed as follows:

- two of the inputs with identity function, *TCR* and *CD28*, are kept in singleton blocks,
- variables with stable function *true* belong to one block,
- variables with stable function *false* belong to another block, and
- we define one more block containing *TLR5* and all variables that belong to its equivalent class in the case of maximal reduction i.e. {*TLR5, TICAM1, PIK3AP1, MyD88, IRAK1, TRAF6, TAB, TAK1, TAK1c, IRAK1, MAP2K3, MAP2K7*}-the blue chain of variables (Fig. 9 top).

We call the reduced BN obtained by the first initial partition *refined reduced model I*.

The second initial partition that we consider is similar to the first but one subtle differentiation: the variable *MAP2K3* is kept in singleton block. The reduced BN that results from this initial partition, is called *refined reduced model II*. The results of our study in this model is summarized in Table 4 . We present the number of variables (*Size*), the number of *Attractors*, and the time needed for reduction (*Reduction (s)*) and attractor identification (*Analysis (s)*).

*Interpretation* As we have seen before, attractor identification is intractable in the original and the ID-reduced BN whereas we can identify two attractors in the case of maximal reduction. Attractor identification in the refined reduced

<i>Model</i>	<i>Size</i>	<i>Attractors</i>	<i>Analysis (s)</i>	<i>Reduction (s)</i>
<i>Original</i>	128	—Time Out—		-
<i>Input-distinguished</i>	116	—Time Out—		2.058
<i>Refined Reduced II</i>	98	8	9349.577	2.096
<i>Refined Reduced I</i>	97	8	1103.912	1.833
<i>Maximal</i>	95	2	29.336	1.958

Table 4: The results of the TCR-TLR merged BN for different reduced versions of the original model.

models is still feasible wherein we find more attractors than in the case of maximal reduction. We should highlight that reducing the TCR-TLR merged BN by just one variable decreases attractor identification time by several orders of magnitude (see *Analysis time* in the case of *Refined Reduced Models*). The computation of the BBE-reduced BN took less than 3 seconds in all cases. To sum up, initializing Algorithm 1 with alternative initial partitions derived from the results of the maximal and ID reduction enables us to explore richer behaviours of the original model.

## C.2 Mitogen-Activated Protein Kinase (MAPK) network

In this Section, we obtain a refined reduced model of the MAPK BN using results from the maximal and the ID reduced model. The original MAPK BN [26] consists of 53 variables, 4 inputs and has 40 attractors. We performed ID BBE-reduction and found the following equivalence classes:  $\{JNK, p38\}$ ,  $\{SMAD, TAK1\}$ ,  $\{ATF2, JUN, MAX, PPP2CA\}$ ,  $\{ELK1, MSK\}$ ,  $\{RSK, SPRY\}$ . The classes are displayed in the up part of Fig. 11 : Backward equivalent variables are represented with colored boxes and colored boxes that belong to the same class have the same background. Variables in white background belong to singleton classes.

*ID Reduction* The ID reduced MAPK BN has 46 variables and 40 attractors. Note that all attractors are preserved. This is a trivial consequence from the fact that (i) the number of attractors is the same, and (ii) the STG of the reduced BN is a subgraph of the STG of the original BN (isomorphism Lemma 2). The BBE-reduction is consistent with [11], where the authors transformed the BN to a system of ordinary differential equations, and reduced with backward differential equivalence.

*Maximal Reduction* The bottom part of Fig. 11 displays the MAPK BN and its equivalence classes after performing the maximal reduction. Algorithm 1 found the following equivalence classes:  $\{JNK, p38\}$ ,  $\{SMAD, TGFBR, ATM, TAOK, EGFR\_stimulus, FGFR3\_stimulus, TGFBR\_stimulus, DNA\_damage, TAK1\}$ ,  $\{ATF2, JUN, MAX, PPP2CA\}$ ,  $\{ELK1, MSK\}$ ,  $\{RSK, SPRY\}$ . BoolSim computes 17 attractors in this case which means that the number of attractors is not preserved. In contrast with [34], the preserved attractors are pure in the original

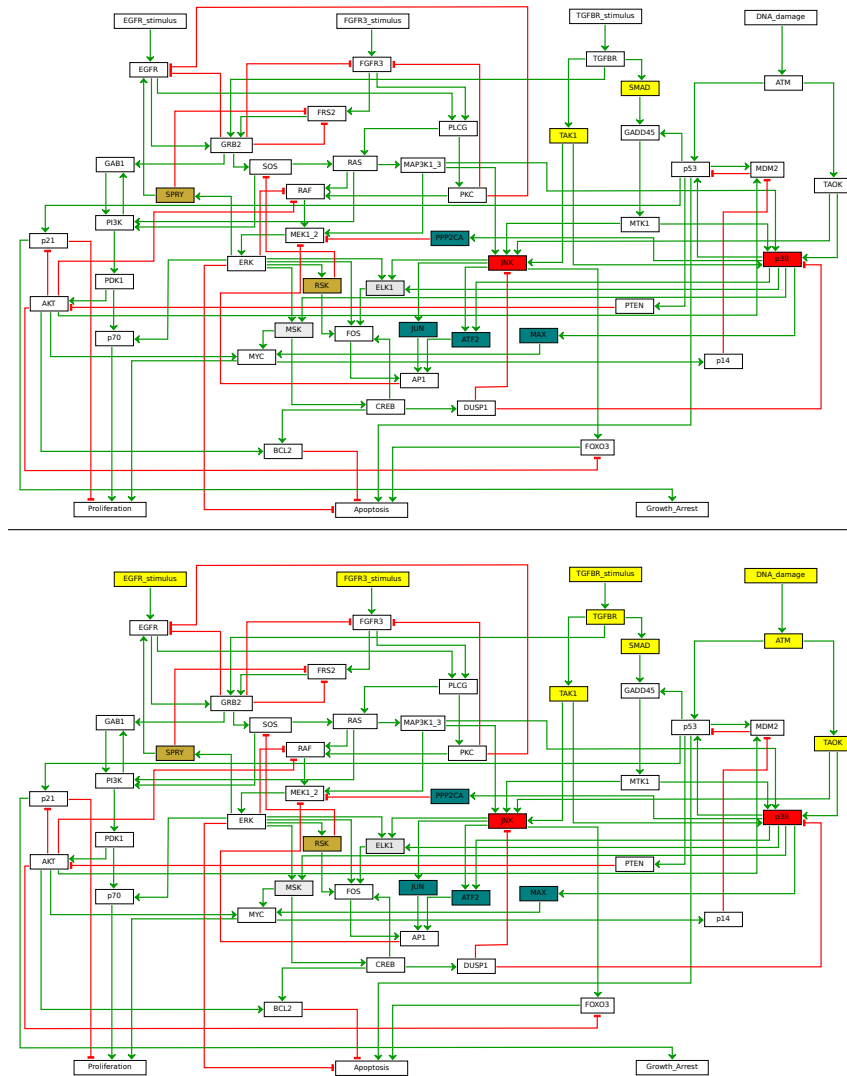


Fig. 11: Up: The MAPK BN with input-distinguishing BBE-variables having the same background color. Bottom: The MAPK BN with maximal-reduction BBE-variables having the same background color. Variables with white background belong to singleton classes.

network in the sense that the isomorphism of Lemma 2 translates the attractors of the reduced to the original BN.

*Refined Reduction* Based on observations gained from the maximal and the ID reduction, we specify the following partition:  $\{EGFR\_stimulus\}$ ,  $\{FGFR3\_stimulus\}$ ,  $\{TGFBR\_stimulus, TGFBR, TAK1, SMAD\}$ ,  $\{DNA\_damage, ATM, TAOK\}$ , and one block containing all the remaining variables. In other words, we keep 2 of the inputs ( $\{EGFR\_stimulus\}$ ,  $\{FGFR3\_stimulus\}$ ) still in singleton sets, while we define two more blocks with each one containing one input and the input’s BBE-variables found in the maximal reduction. We expect that the reduced BN, which now contains 42 variables (79, 25% of the original size), preserves more properties. Indeed, the refined reduced BN has all 40 attractors of the original BN. The results of our study in this model is summarized in the following Table 5 . We present the number of variables (*Size*), the number of *Attractors*, and the time needed for reduction (*Reduction (s)*) and attractor identification (*Analysis (s)*).

<i>Model</i>	<i>Size</i>	<i>Attractors</i>	<i>Analysis (s)</i>	<i>Reduction (s)</i>
<i>Original</i>	53	40	16.501	-
<i>Input-distinguished</i>	46	40	14.480	0.848
<i>Refined Reduced</i>	42	40	12.115	1.202
<i>Maximal</i>	39	17	2.471	1.018

Table 5: The results of the MAPK BN for different reduction versions of the original model.

### C.3 T cell granular lymphocyte (T-LGL) leukemia BN

T-LGL BN was originally introduced in [52] and refers to the disease T-LGL leukemia which features a clonal expansion of antigen-primed, competent, cytotoxic T lymphocytes (CTL). The T-LGL BN is a signalling pathway, constructed empirically through extensive literature review, and determines the survival of CTL. The ID reduction and the maximal reduction are depicted in the top part and the bottom part of Fig. 12 respectively. The original BN consists of 60 variables, and has 264 attractors.

In the case of ID reduction, the variables *FasT*, *A20*, *TNF* and *RANTES* are BBE-equivalent so we can collapse them into a single variable. The ID reduced BN has 57 variables, and 264 attractors. Since the number of attractors is the same, and the STG of the reduced BN is a subgraph of the STG of the original BN, the asymptotic dynamics are preserved. The bottom part of Fig. 12 refers to the maximal BBE. In this case, we have two equivalence classes: the one found in ID BBE, and one consisted of all the input variables. On the other hand, the maximal reduced BN has 52 variables and 6 attractors. This means that some attractors are lost.

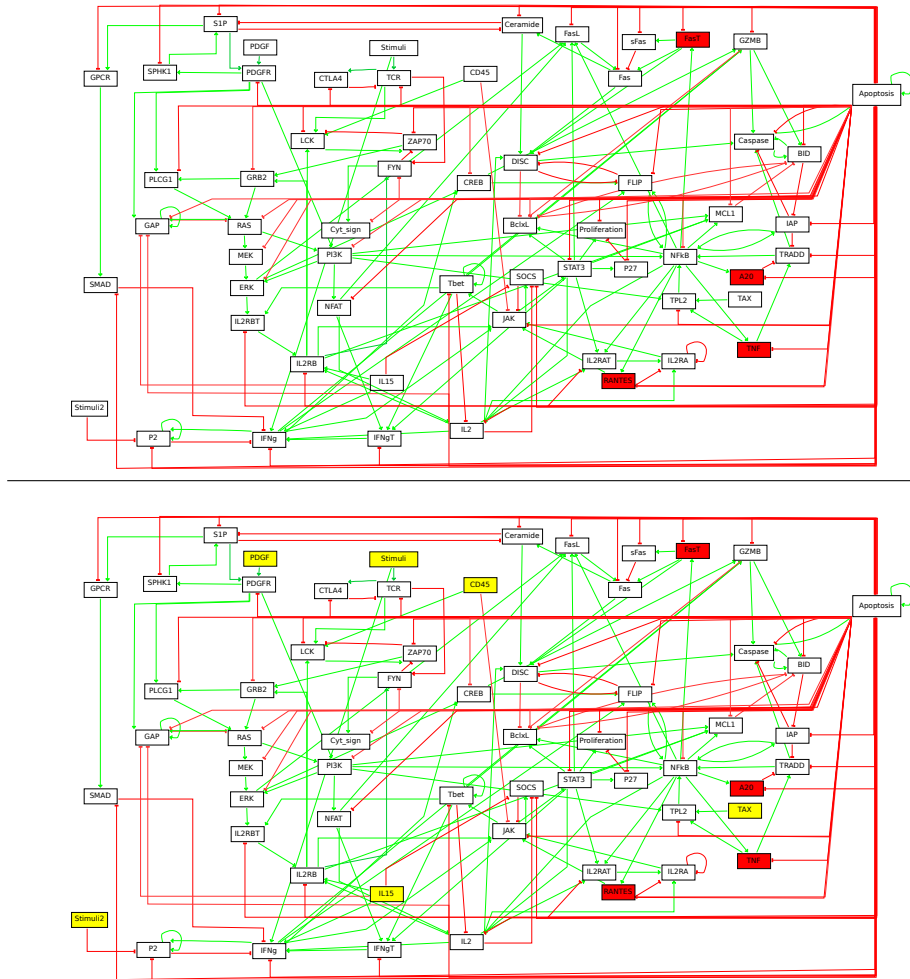


Fig. 12: Up: The T-LGL BN with input-distinguishing BBE-variables having the same background color. Bottom: The T-LGL BN with maximal-reduction BBE-variables having the same background color. Variables with white background belong to singleton classes.

In [52], the authors considered the asynchronous schema and presented a variable specified analysis. Specifically, their analysis determined which variables are sufficient to induce all of known signalling abnormalities in leukemic T-LGL, which variables are important for the survival of leukemic T-LGL, and which variables are constantly active in leukemic T-LGL. Notably, permanent activation of the variables  $IL - 15$  and  $PDGF$  is sufficient to produce all of the known deregulations and signalling abnormalities. For this reason, we consider as reasonable initial partition one wherein  $IL - 15$  and  $PDGF$  belong to the same block, other input variables belong to singleton blocks, and non-input variables belong to one block. In this case, the refined reduced BN has 56 variables and 120 attractors. In contrast with the maximal reduced and the original BN which have 264 attractors, the BN reduced with this reasonable initial partition discards 144 attractors which are irrelevant for this kind of analysis. The results of our study on this model is summarized in the following Table 6 . We present the number of variables (*Size*), the number of *Attractors*, and the time needed for reduction (*Reduction (s)*) and attractor identification (*Analysis (s)*).

<i>Model</i>	<i>Size</i>	<i>Attractors</i>	<i>Analysis (s)</i>	<i>Reduction (s)</i>
<i>Original</i>	60	264	123.431	-
<i>Input-distinguished</i>	57	264	85.999	0.843
<i>Refined Reduced</i>	56	120	55.049	1.816
<i>Maximal</i>	52	6	2.489	0.999

Table 6: The results of the T-LGL BN for different reduction versions of the original model.

## D Speed-ups on STG generation in BBE-reduced models

*Hypothesis* We hope to drastically reduce the time needed for STG generation. Furthermore, we claim that our technique may be utilized for STG visualization since reducing a BN only by one variable results in reducing its corresponding STG by 50%.

*Configuration* We reduced the original BN with both ID and maximal BBE-reduction. We observed that PyBoolNet failed to generate the STG of BNs that have more than 25 variables. Hence, we restricted our experiments to all BNs with less variables. PyBoolNet generates the STG within several minutes for BNs between 21 and 25 variables, and within a minute for BNs with up to 20 variables. We did not consider BNs with less than 9 variables since the generation and visualization of the full STG is feasible and computationally costless. We present the results in Table 7:

Model	Original model		Input-distinguished Reduced model			Maximal Reduced model		
	Size	STG generation(s)	Reduction (s)	Size	STG generation(s)	Reduction (s)	Size	STG generation(s)
B7	33	out of memory	0.585	27	out of memory	0.608	25	out of memory
B9	28	out of memory	0.449	25	out of memory	0.416	20	52.8
B10	26	out of memory	0.227	23	457	0.145	4	0.006
B11	24	984	0.243	23	475	0.207	9	0.280
B12	24	987	0.349	21	102	0.121	4	0.050
B13	23	455	0.302	22	226	0.176	8	0.164
B14	20	55.6	0.497	15	2.11	0.408	13	0.302
B15	18	11.6	0.209	18	11.6	0.182	8	0.007
B16	18	14.300	—NO INPUTS—			0.449	17	6.760
B17	14	0.867	0.267	14	0.867	0.389	12	0.169
B18	11	0.072	0.327	10	0.064	0.214	9	0.065
B19	10	0.044	0.228	9	0.016	0.303	9	0.016
B20	10	0.172	0.283	8	0.044	0.202	8	0.044
B21	9	0.015	—NO INPUTS—			0.279	7	0.005
B22	9	0.025	—NO INPUTS—			0.237	7	0.003
M9	57	out of memory	0.791	57	out of memory	0.260	11	0.233
M16	37	out of memory	0.907	37	out of memory	0.454	14	1.360
M17	36	out of memory	0.413	35	out of memory	0.516	21	136
M20	34	out of memory	0.364	32	out of memory	0.383	15	2.68
M21	30	out of memory	0.421	30	out of memory	0.238	14	1.37
M22	24	1212	0.251	23	1043	0.219	12	0.172
M23	21	130	0.273	21	130	0.326	18	14.6
M24	19	31	0.109	19	31	0.153	7	0.463
M25	19	28.3	0.210	19	28.3	0.243	12	0.609
M26	19	30.1	0.249	18	13.9	0.356	17	6.320
M27	18	14.2	0.161	18	14.2	0.194	10	0.260
M28	16	3.34	0.189	16	3.34	0.266	13	1.54
M29	16	3.15	0.101	16	3.15	0.096	5	0.028
M30	15	1.59	0.187	15	1.59	0.235	13	0.303
M31	14	0.883	0.178	14	0.883	0.203	13	0.444
M32	12	0.156	0.168	12	0.156	0.137	8	0.010
M33	10	0.032	0.098	10	0.032	0.044	8	0.007

Table 7: Time needed for model reduction and STG generation of the original and the reduced BN. The running times are coming from one run and the computation of the BBE-reduced BNs take no more than 1 second in the worst cases.

*Results* PyBoolNet failed to generate the STG of the original B9 [4]. This was done within a minute after applying maximal BBE-reduction. For BNs between 20 and 25 variables, our method drastically decreased the STG generation time: The STG of the ID BN needs on average 25% of the time for the generation of the full STG, and the maximal BN needs less than 1% of the time needed for the generation of the full STG. For BNs with less than 20 variables the reduction may be computationally effective in several cases (see B15 and B16 in Table 7).

*Interpretation* We should note that our method (i) may render the analysis of large BN models tractable in many cases (like B9, M9, and M21) and (ii) facilitates STG visualization. BBE-reduction constitutes a useful method for generating pure segments of the original state space. According to the isomorphism Lemma 2, the STG of the reduced BN constitutes a subgraph of the STG of the original BN resulting from it after the collapse of a BBE-class into one variable component. In other words, our reduction method provides a pure image of the

state space of the original BN. We utilize these results in Section 4.2 wherein we conduct an attractor based analysis.